NAMT
92-043

Numerical solution of diffraction problems: a method of variation of boundaries II. Dielectric gratings, Padé approximants and singularities

Oscar P. Bruno
Georgia Institute of Technology
Fernando Reitich
Carnegie Mellon University

Research Report No. 92-NA-043

DECEMBER 1992

Sponsors

U.S. Army Research Office
Research Triangle Park
NC 27709

National Science Foundation
1800 G Street, N.W.
Washington, DC 20550

Numerical solution of diffraction problems: a method of variation of boundaries II. Dielectric gratings, Padé approximants and singularities

Oscar P. Bruno* Fernando Reitich†

Abstract

We have recently introduced a method of variation of boundaries for the solution of diffraction problems. This method, which is based on a theorem of analyticity of the electromagnetic field with respect to variations of the interfaces, has been successfully applied in problems of diffraction of light by perfectly conducting gratings. In this paper we continue our investigation of diffraction problems. Using our previous results on analytic dependence with respect to the grating groove-depth, we present a new numerical algorithm which applies to dielectric gratings. We also incorporate Padé approximation in our numerics. This addition enlarges the domain of applicability of our methods, and it results in computer codes which can predict more accurately the response of diffraction gratings in the resonance region. In many cases, results are obtained which are several orders of magnitude more accurate than those given by other methods available at present, such as the integral or differential formalisms.

We present a variety of numerical applications, including examples for several types of grating profiles and for wavelengths of light ranging from microwaves to ultraviolet, and we compare our results with experimental data. We also use Padé approximants to gain insight on the analytic structure and the spectrum of singularities of the fields as functions of the groove-depth. Finally, we discuss some connections between Padé approximation and another summation mechanism, enhanced convergence, which we introduced earlier. It is argued that, provided certain numerical difficulties can be overcome, the performance of our algorithms could be further improved by a combination of these summation methods.

*School of Mathematics, Georgia Institute of Technology, Atlanta, Georgia 30332-0160
†Department of Mathematics, Carnegie Mellon University, Pittsburgh, Pennsylvania 15213-3890

1 Introduction

We have recently introduced a method of variation of boundaries for the solution of diffraction problems [5]. This method, which is based on a theorem of analyticity of the electromagnetic field with respect to variations of the interfaces, has been successfully applied in problems of diffraction of light by perfectly conducting gratings [6]. In this paper we continue our investigation of diffraction problems. Using our previous results on analytic dependence with respect to the grating groove-depth, we present a new numerical algorithm which applies to dielectric gratings. We also incorporate Padé approximation in our numerics. This addition enlarges the domain of applicability of our methods, and it results in computer codes which can predict more accurately the response of diffraction gratings in the resonance region. In many cases, results are obtained which are several orders of magnitude more accurate than those given by other methods available at present, such as the integral or differential formalisms.

For several decades perturbation methods have been considered inadequate for the treatment of problems of wave scattering by gratings, and only few of the many discussions in this area have been based on perturbative techniques. Low order perturbative approaches include those of Rayleigh [23] and, much more recently, Wait [27], while, for higher order methods, the literature seems to reduce to the work of Meecham [19]. Low order methods are only appropriate for very shallow gratings and, in particular, they cannot be applied to gratings in the resonance region (i.e., gratings whose height to period ratio is comparable to the wavelength to period ratio) [17, 24]. The approach of Meecham, on the other hand, produces the solution as a Neumann series whose n-th term is given by an n-fold convolution of the Green's function. This method, which has not been implemented numerically, was thought to be mathematically incorrect [25], and dismissed. Attention then focused on integral, differential and modal methods (see [22, 11, 14]).

Uretsky [25, p. 411] objected to Meecham's approach, and conjectured that the electromagnetic fields for a grating do not continue analytically to the fields for a flat interface. Uretsky's conjecture was based on a certain integral expression related to the fields which appears to become meaningless as the groove depth takes complex values. As we have said, however, the fields *are* analytic functions of the grating groove depth [5]. Furthermore, simple *algebraic* recursive formulae can be given which permit one to calculate *in closed form* the diffractive amplitudes *to arbitrary order in the groove depth*, without recourse to calculation of iterated integrals. An algorithm based on the analyticity properties of the fields can, therefore, be devised. A final complication arises as the calculated power series for the diffracted amplitudes converge for relatively shallow gratings only. This difficulty, which is not to be confused with restrictions to shallow gratings that are inherent in low order methods, can be circumvented as we shall show below (see also [6]). Thus, efficient algorithms based on perturbation theory can be obtained. In fact, higher order perturbation methods can also be applied to three dimensional biperiodic gratings, and some preliminary experiments indicate that they can exhibit a very good performance in this problem in which other methods have had limited success. Indeed, for sinusoidal biperiodic gratings, and for a given height to period ratio, our methods yield results with the same order or even better accuracy than in the corresponding singly periodic sinusoidal case. A complete discussion of our approach in a doubly periodic setting will be presented elsewhere.

This paper is organized as follows. Section 2 contains a description of theoretical and numerical aspects of our method; the basic recursive relations for dielectric gratings are given in §2.3. In §3 we present a variety of numerical applications, including examples for several types of grating profiles and for wavelengths of light ranging from microwaves to ultraviolet, and we compare our results with experimental data. Finally, a discussion of the analytic structure of the electromagnetic field and some remarks on the connections between the methods of Padé approximation and enhanced convergence as they apply to our problem are presented in §4. Enhanced convergence is an alternative summation mechanism that we introduced in [6]. It uses conformal transformations to produce a rearrangement of the singularities of the fields in the complex plane which is favorable for the summation of a truncated series. It is argued that, provided certain numerical difficulties can be overcome, the performance of our algorithms could be further improved by a combination of these summation methods.

2 Analytic dependence, recursive formulae and numerics

In this section we introduce the basic elements of our algorithm. In §2.1 we set our notation, and in §2.2 we review our results on the analyticity properties of the electromagnetic field with respect to variations of the grating profile. In §2.3 we derive recursive formulae for the coefficients of the power series expansion of the diffractive amplitudes. The algebra in this derivation is somewhat involved, but it results in formulae that are easy to implement numerically. In §2.4 we indicate how the power series can be used to extract the values of the efficiencies.

2.1 Preliminaries

Let us consider a periodic function f of period d, and the grating profile

$$y = f_\delta(x) = \delta f(x),$$

which separates the regions $y > f_\delta(x)$ and $y < f_\delta(x)$ (δ is a real number). These regions are assumed to be filled by materials of dielectric constants ϵ^+ and ϵ^- respectively. The permeability of the dielectrics is assumed to equal μ_0, the permeability of vacuum. Assume the grating is illuminated by either a TE or TM polarized incident beam

$$\vec{E}^i = \vec{A}e^{i\alpha x - i\beta y}e^{(-i\omega t)}$$
$$\vec{H}^i = \vec{B}e^{i\alpha x - i\beta y}e^{(-i\omega t)}.$$

In either case of polarization, one of the fields $\vec{E}$ or $\vec{H}$ remains parallel to the grooves, and is, therefore, determined by a single scalar quantity $u = u(x, y, \delta)$ (equal to the transverse component

E_z of $\vec{E}$ in the TE case, and to the transverse component H_z of $\vec{H}$ in the TM case). The functions $u = u^{\pm}$ satisfy Helmholtz equations

$$\Delta u^{\pm} + (k^{\pm})^2 u^{\pm} = 0 \ , \ \text{in}\, \Omega^{\pm} = \{\pm y > \pm\delta f(x)\}\,,$$

and the boundary conditions

$$\begin{aligned} u^+ - u^- &= -e^{i\alpha x - i\beta\delta f(x)} \ , \ \text{ on } \ y = \delta f(x)\,, \\ \frac{\partial u^+}{\partial n_\delta} - C_0^2 \frac{\partial u^-}{\partial n_\delta} &= -\frac{\partial}{\partial n_\delta}(e^{i\alpha x - i\beta\delta f(x)}) \ , \ \text{ on } \ y = \delta f(x). \end{aligned} \tag{1}$$

Here we have put $k^{\pm} = \omega\sqrt{\mu_0 \epsilon^{\pm}}$,

$$C_0 = \begin{cases} 1 & \text{for TE polarization,} \\ \left(\frac{k^+}{k^-}\right) & \text{for TM polarization,} \end{cases}$$

and $n_\delta = n_\delta(x, \delta f(x))=$ unit normal to $\{y = \delta f(x)\}$.

The periodicity of the structure leads to certain properties of periodicity in the fields, which can, therefore, be expanded in Fourier series. The resulting expansions, the so-called Rayleigh series, incorporate also conditions of radiation at infinity. Set

$$K = \frac{2\pi}{d} \ , \ \alpha_n = \alpha + nK \ , \ \alpha_n^2 + (\beta_n^{\pm})^2 = (k^{\pm})^2\,,$$

where $\beta_n^{\pm}$ is determined by $\mathrm{Im}(\beta_n^{\pm}) > 0$ or $\beta_n^{\pm} \geq 0$. The Rayleigh expansion in the region Ω^+, which is necessarily convergent for $y > y_M = \max \delta f$, is given by

$$u^+ = \sum_{n=-\infty}^{\infty} B_n^+ e^{i\alpha_n x + i\beta_n^+ y}.$$

In Ω^- we have the Rayleigh expansion,

$$u^- = \sum_{n=-\infty}^{\infty} B_n^- e^{i\alpha_n x - i\beta_n^- y},$$

which converges for $y < y_m = \min \delta f$. It is to be noted that these expansions can be divergent in the region inside the grooves [20].

Only finitely many of the Rayleigh amplitudes B_n correspond to propagating modes, as the numbers β_n have nonzero imaginary part for n large enough. For loseless gratings, the principle of conservation of energy yields a useful relation between the amplitudes of the propagating modes. Indeed, in case the constants $k^{\pm}$ are real, this "energy balance criterion" is given by

$$\sum_{n\in U^+} \beta_n^+ |B_n^+|^2 + C_0^2 \sum_{n\in U^-} \beta_n^- |B_n^-|^2 = \beta_0^+ (= \beta)$$

where $U^{\pm}$ are the finite sets

$$U^{\pm} \equiv \{n : \beta_n^{\pm} > 0\}\,.$$

Equivalently, we obtain the relation

$$\sum_{n\in U^+} e_n^+ + C_0^2 \sum_{n\in U^-} e_n^- = 1$$

for the *efficiencies*

$$e_n^\pm = \beta_n^\pm |B_n^\pm|^2/\beta_0^+$$

of the propagating modes. For perfectly conducting gratings, we only have reflected efficiencies, and in this case the energy balance criterion reads

$$\sum_{n\in U^+} e_n = 1. \tag{2}$$

2.2 The theory

As we said, our algorithm is based on a property of analyticity of the field $u = u(x, y, \delta)$ with respect to the parameter δ. More precisely, under the assumption that the function $f(x)$ is analytic, we have established the following results [5]:

1. Given $\delta_0 \in \mathbf{R}$ and y_0 above (or below) the profile $y = \delta_0 f(x)$, the function $u = u(x, y, \delta)$ is an analytic function of its three variables for y sufficiently close to y_0 and δ sufficiently close to δ_0.
2. The functions
$$u^\pm(x, \delta f(x), \delta) \text{ and}$$
$$\frac{\partial u^\pm}{\partial n_\delta(x, \delta f(x))}(x, \delta f(x), \delta)$$
are analytic with respect to x and δ.
3. Given $\delta_0 \in \mathbf{R}$ the functions $u^\pm$ are analytic with respect to x, y and δ for δ close to δ_0 and y close to the curve $y = \delta_0 f(x)$ (notice that this implies, in particular, that the functions u^+ and u^- can be extended analytically across the interface).

From points 1) and 3) above, it follows that the functions $u^\pm$ can be expanded in series in powers of δ

$$u^\pm(x, y, \delta) = \sum_{n=0}^{\infty} u_n^\pm(x, y)\delta^n \tag{3}$$

which converge for δ small enough. The functions $u_n^\pm$ satisfy Helmholtz equations

$$\Delta u_n^\pm + (k^\pm)^2 u_n^\pm = 0 \text{ in } \{ (x, y) \, : \, \pm y > 0 \}$$

and conditions of radiation at infinity. They also satisfy boundary conditions at $y = 0$ which are obtained recursively by differentiation of equations (1) with respect to δ at $\delta = 0$. Such differentiations and use of the chain rule are permissible, as it follows from points 2) and 3) above.

2.3 Recursive Formulae

To obtain recursive formulae for the Taylor coefficients of the diffractive amplitudes, we begin by finding the transmission conditions the functions $u_n^\pm$ satisfy at $y=0$. Differentiation of the first equation in (1) n times with respect to δ at $\delta = 0$ yields the relation

$$\begin{aligned}\textstyle\sum_{k=0}^{n} \frac{f(x)^{n-k}}{(n-k)!}\left(\frac{\partial^{n-k}}{\partial y^{n-k}}\left(\frac{1}{k!}\frac{\partial^k u^+}{\partial \delta^k}\right)(x,0,0) - \frac{\partial^{n-k}}{\partial y^{n-k}}\left(\frac{1}{k!}\frac{\partial^k u^-}{\partial \delta^k}\right)(x,0,0)\right) \\ = -\frac{(-i\beta)^n}{n!} f(x)^n e^{i\alpha x}.\end{aligned} \tag{4}$$

Since

$$n_\delta = \frac{1}{\sqrt{1+\delta^2 f'(x)^2}}(-\delta f'(x), 1),$$

the second equation in (1) can be written in the form

$$\begin{aligned}-\delta f'(x)\left(\frac{\partial u^+}{\partial x} - C_0^2\frac{\partial u^-}{\partial x}\right) + \left(\frac{\partial u^+}{\partial y} - C_0^2\frac{\partial u^-}{\partial y}\right) \\ = \left(\delta f'(x) i\alpha + i\beta\right) e^{i\alpha x - i\beta\delta f(x)}.\end{aligned}$$

Thus, n differentiations with respect to δ yield

$$\begin{aligned}\textstyle\sum_{k=0}^{n} \frac{f(x)^{n-k}}{(n-k)!}\left(\frac{\partial^{n-k+1}}{\partial y^{n-k+1}}\left(\frac{1}{k!}\frac{\partial^k u^+}{\partial \delta^k}\right)(x,0,0) - C_0^2\frac{\partial^{n-k+1}}{\partial y^{n-k+1}}\left(\frac{1}{k!}\frac{\partial^k u^-}{\partial \delta^k}\right)(x,0,0)\right) \\ -\textstyle\sum_{k=0}^{n-1} \frac{f'(x)f(x)^{n-k-1}}{(n-k-1)!}\left(\frac{\partial^{n-k}}{\partial y^{n-k-1}\partial x}\left(\frac{1}{k!}\frac{\partial^k u^+}{\partial \delta^k}\right)(x,0,0) - C_0^2\frac{\partial^{n-k}}{\partial y^{n-k-1}\partial x}\left(\frac{1}{k!}\frac{\partial^k u^-}{\partial \delta^k}\right)(x,0,0)\right) \\ = \frac{1}{n!}\left(i\alpha n(-i\beta)^{n-1} f'(x) f(x)^{n-1} - (-i\beta)^{n+1} f(x)^n\right) e^{i\alpha x}.\end{aligned} \tag{5}$$

From (3) we have

$$u_k^\pm(x,y) = \frac{1}{k!}\frac{\partial^k u^\pm}{\partial \delta^k}(x,y,0) \tag{6}$$

so that equations (4), (5) can be made to read

$$u_n^+ - u_n^- = -\frac{(-i\beta)^n}{n!} f^n e^{i\alpha x} - \sum_{k=0}^{n-1} \frac{f^{n-k}}{(n-k)!}\left(\frac{\partial^{n-k} u_k^+}{\partial y^{n-k}} - \frac{\partial^{n-k} u_k^-}{\partial y^{n-k}}\right) \tag{7}$$

and

$$\begin{aligned}\frac{\partial u_n^+}{\partial y} - C_0^2\frac{\partial u_n^-}{\partial y} &= \frac{1}{n!}\left(i\alpha n(-i\beta)^{n-1}(f' f^{n-1}) - (-i\beta)^{n+1} f^n\right) e^{i\alpha x} \\ &+ \sum_{k=0}^{n-1} \frac{(f' f^{n-k-1})}{(n-k-1)!}\left(\frac{\partial^{n-k} u_k^+}{\partial x \partial y^{n-k-1}} - C_0^2 \frac{\partial^{n-k} u_k^-}{\partial x \partial y^{n-k-1}}\right) \\ &- \sum_{k=0}^{n-1} \frac{f^{n-k}}{(n-k)!}\left(\frac{\partial^{n-k+1} u_k^+}{\partial y^{n-k+1}} - C_0^2 \frac{\partial^{n-k+1} u_k^-}{\partial y^{n-k+1}}\right).\end{aligned} \tag{8}$$

Because the functions $u_n^\pm$ in (3) are quasi-periodic solutions of the Helmholtz equation in a semi-plane, they can be expanded in Rayleigh series

$$u_n^\pm(x,y) = \sum_{r=-\infty}^{\infty} d_{n,r}^\pm e^{i\alpha_r x \pm i\beta_r^\pm y} \tag{9}$$

similar to those which represent the functions $u^{\pm}(x,y,\delta)$ for $\pm y > \pm\delta f(x)$:

$$u^{\pm}(x,y,\delta) = \sum_{r=-\infty}^{\infty} B_r^{\pm}(\delta) e^{i\alpha_r x \pm i\beta_r^{\pm} y}.$$

It is plain from (6) that

$$d_{n,r}^{\pm} = \frac{1}{n!}\frac{d^n B_r^{\pm}}{d\delta^n}(0),$$

so that we have the Taylor series

$$B_r^{\pm}(\delta) = \sum_{n=0}^{\infty} d_{n,r}^{\pm}\delta^n \tag{10}$$

for the Rayleigh coefficients $B_r^{\pm}$. Our approach is based on evaluation of the Taylor series (10), whose coefficients $d_{n,r}^{\pm}$ can be obtained recursively. To obtain a recursive formula, let

$$f(x) = \sum_{r=-F}^{F} C_{1,r} e^{iKrx}\ ,\ K = \frac{2\pi}{d}\ ,$$

be the Fourier expansion of the function f (with finite or infinite F) and let $C_{l,r}$ denote the Fourier coefficients of the function $f(x)^l/l!$

$$\frac{f(x)^l}{l!} = \sum_{r=-lF}^{lF} C_{l,r} e^{iKrx}.$$

Then, substitution in (7), (8) of $u_n^{\pm}$ and the spatial derivatives of $u_k^{\pm}$ as calculated from (9) yields the coefficients $d_{n,r}^{\pm}$ in terms of the coefficients $d_{k,r}^{\pm}$ $(k < n)$ and $C_{l,r}$. Indeed, from (7) we have

$$\begin{aligned}\textstyle\sum_{r=-\infty}^{\infty}(d_{n,r}^{+} - d_{n,r}^{-})e^{i\alpha_r x} &= -(-i\beta)^n \textstyle\sum_{r=-nF}^{nF} C_{n,r}e^{i\alpha_r x}\\ -\textstyle\sum_{k=0}^{n-1}\left(\sum_{r=-(n-k)F}^{(n-k)F} C_{n-k,r}e^{iKrx}\right)&\left[\textstyle\sum_{r=-\infty}^{\infty}\left((i\beta_r^{+})^{n-k}d_{k,r}^{+} - (-i\beta_r^{-})^{n-k}d_{k,r}^{-}\right)e^{i\alpha_r x}\right]\end{aligned} \tag{11}$$

and, since

$$\frac{1}{n!}(nf'(x)f(x)^{n-1}) = \frac{d}{dx}\left(\frac{f^n}{n!}\right) = \sum_{r=-nF}^{nF} C_{n,r}iKre^{iKrx},$$

equation (8) becomes

$$\begin{aligned}\textstyle\sum_{r=-\infty}^{\infty}\left(i\beta_r^{+}d_{n,r}^{+} + C_0^2 i\beta_r^{-}d_{n,r}^{-}\right)e^{i\alpha_r x} &= \textstyle\sum_{r=-nF}^{nF} C_{n,r}\left(i\alpha(-i\beta)^{n-1}(iKr) - (-i\beta)^{n+1}\right)e^{i\alpha_r x}\\ &+\textstyle\sum_{k=0}^{n-1}\left(\sum_{r=-(n-k)F}^{(n-k)F} C_{n-k,r}iKre^{iKrx}\right)\left[\sum_{r=-\infty}^{\infty}\left((i\beta_r^{+})^{n-k-1}(i\alpha_r)d_{k,r}^{+}\right.\right.\\ &\qquad\left.\left.-C_0^2(-i\beta_r^{-})^{n-k-1}(i\alpha_r)d_{k,r}^{-}\right)e^{i\alpha_r x}\right]\\ &-\textstyle\sum_{k=0}^{n-1}\left(\sum_{r=-(n-k)F}^{(n-k)F} C_{n-k,r}e^{iKrx}\right)\left[\sum_{r=-\infty}^{\infty}\left((i\beta_r^{+})^{n-k+1}d_{k,r}^{+}\right.\right.\\ &\qquad\left.\left.-C_0^2\,(-i\beta_r^{-})^{n-k+1}d_{k,r}^{-}\right)e^{i\alpha_r x}\right].\end{aligned} \tag{12}$$

We now rewrite the right hand sides of (11) and (12) so as to display the coefficient of each particular mode. The right hand side of (11) is equal to

$$
\begin{gathered}
-\sum_{r=-nF}^{nF}(-i\beta)^n C_{n,r} e^{i\alpha_r x} \\
-\sum_{k=0}^{n-1}\sum_{q=-\infty}^{\infty}\sum_{p=-(n-k)F}^{(n-k)F} C_{n-k,p}\left((i\beta_q^+)^{n-k} d_{k,q}^+ - (-i\beta_q^-)^{n-k} d_{k,q}^-\right) e^{iKpx} e^{i\alpha_q x}.
\end{gathered}
$$

Since

$$
e^{iKpx}e^{i\alpha_q x} = e^{i\alpha_{p+q} x},
$$

changing p by $r-q$ in the inner sum gives

$$
\begin{gathered}
-\sum_{r=-nF}^{nF}(-i\beta)^n C_{n,r} e^{i\alpha_r x} \\
-\sum_{k=0}^{n-1}\sum_{q=-\infty}^{\infty}\sum_{r=q-(n-k)F}^{q+(n-k)F} C_{n-k,r-q}\left((i\beta_q^+)^{n-k} d_{k,q}^+ - (-i\beta_q^-)^{n-k} d_{k,q}^-\right) e^{i\alpha_r x} \\
= -\sum_{r=-nF}^{nF}(-i\beta)^n C_{n,r} e^{i\alpha_r x} \\
-\sum_{r=-\infty}^{\infty}\left[\sum_{k=0}^{n-1}\sum_{q=r-(n-k)F}^{r+(n-k)F} C_{n-k,r-q}\left((i\beta_q^+)^{n-k} d_{k,q}^+ - (-i\beta_q^-)^{n-k} d_{k,q}^-\right)\right] e^{i\alpha_r x}.
\end{gathered} \tag{13}
$$

Now, it can be checked inductively that

$$
d_{k,q}^{\pm} = 0 \quad \text{if } |q| > kF.
$$

In other words, in the last term of (13), the sum over q can be restricted to $-kF \le q \le kF$ and therefore the sum in r reduces to a sum for $-nF \le r \le nF$. Thus, (11) is equivalent to

$$
\begin{gathered}
\sum_{r=-nF}^{nF}(d_{n,r}^+ - d_{n,r}^-)e^{i\alpha_r x} = -\sum_{r=-nF}^{nF}\Big\{(-i\beta)^n C_{n,r} \\
+\sum_{k=0}^{n-1}\sum_{q=\max(-kF,r-(n-k)F)}^{\min(kF,r+(n-k)F)} C_{n-k,r-q}\left((i\beta_q^+)^{n-k} d_{k,q}^+ - (-i\beta_q^-)^{n-k} d_{k,q}^-\right)\Big\} e^{i\alpha_r x}.
\end{gathered} \tag{14}
$$

A similar calculation permits us to transform equation (12) into

$$
\begin{gathered}
\sum_{r=-nF}^{nF}\left(i\beta_r^+ d_{n,r}^+ + C_0^2 i\beta_r^- d_{n,r}^-\right) e^{i\alpha_r x} \\
= \sum_{r=-nF}^{nF}\Big\{C_{n,r}(-i\beta)^{n-1}\left((i\alpha)(iKr) - (-i\beta)^2\right) \\
+\sum_{k=0}^{n-1}\sum_{q=\max(-kF,r-(n-k)F)}^{\min(kF,r+(n-k)F)} C_{n-k,r-q}\Big[(iK(r-q))(i\alpha_q)\big((i\beta_q^+)^{n-k-1} d_{k,q}^+ \\
-C_0^2\,(-i\beta_q^-)^{n-k-1} d_{k,q}^-\big) - \left((i\beta_q^+)^{n-k+1} d_{k,q}^+ - C_0^2(-i\beta_q^-)^{n-k+1} d_{k,q}^-\right)\Big]\Big\} e^{i\alpha_r x}.
\end{gathered} \tag{15}
$$

Recursive formulae for the Taylor coefficients $d_{n,r}^{\pm}$ now follow from (14), (15):

$$
\begin{gathered}
d_{n,r}^+ - d_{n,r}^- = -(-i\beta)^n C_{n,r} \\
-\sum_{k=0}^{n-1}\sum_{q=\max(-kF,r-(n-k)F)}^{\min(kF,r+(n-k)F)} C_{n-k,r-q}\left((i\beta_q^+)^{n-k} d_{k,q}^+ - (-i\beta_q^-)^{n-k} d_{k,q}^-\right),
\end{gathered} \tag{16}
$$

$$
\begin{gathered}
i\beta_r^+ d_{n,r}^+ + C_0^2 i\beta_r^- d_{n,r}^- = C_{n,r}(-i\beta)^{n-1}\left((i\alpha)(iKr) - (-i\beta)^2\right) \\
+\sum_{k=0}^{n-1}\sum_{q=\max(-kF,r-(n-k)F)}^{\min(kF,r+(n-k)F)} C_{n-k,r-q}\Big[(iK(r-q))(i\alpha_q)\big((i\beta_q^+)^{n-k-1} d_{k,q}^+ \\
-C_0^2\,(-i\beta_q^-)^{n-k-1} d_{k,q}^-\big) - \left((i\beta_q^+)^{n-k+1} d_{k,q}^+ - C_0^2(-i\beta_q^-)^{n-k+1} d_{k,q}^-\right)\Big].
\end{gathered} \tag{17}
$$

2.4 Numerical implementation

Formulae (16) and (17) allow us to calculate recursively the Taylor coefficients $d^{\pm}_{n,r}$. Note that, for given integers n and r, only some of the coefficients $d^{\pm}_{k,q}$ $(k < n)$ are involved in the computation of $d^{\pm}_{n,r}$. Indeed, to compute $d^{\pm}_{n,r}$ we only need $d^{\pm}_{k,q}$ for $k < n$ and for

$$\max(-kF, r-(n-k)F) \leq q \leq \min(kF, r+(n-k)F).$$

Thus, generation of the coefficients $d^{\pm}_{n,r}$ should be restricted to those which will eventually contribute to the calculation of the diffractive efficiencies to some prescribed order. In order to obtain further reductions in the computation time, one can also truncate the sums by setting $d^{\pm}_{k,q} = 0$ for modes q larger than a certain mode q_0. We refer to [6] for details.

There remains the problem of extracting the values of the Rayleigh coefficients from their Taylor expansions. To do this we use Padé approximation. In our previous paper [6] we used a different summation method, which we called enhanced convergence. This method permitted us to deal with many practical situations, but it is apparent now that better performance results from use of Padé approximants. In §4 we discuss the relations between Padé approximation and the method of enhanced convergence.

The $[L/M]$-Padé approximant of a function

$$B(\delta) = \sum_{n=0}^{\infty} d_n \delta^n \tag{18}$$

is defined (see [2]) as a rational function

$$[L/M] = \frac{a_0 + a_1\delta + \cdots + a_L\delta^L}{1 + b_1\delta + \cdots + b_M\delta^M}$$

whose Taylor series agrees with that of B up to order $L+M+1$. A particular $[L/M]$ approximant may fail to exist but, generically, $[L/M]$ Padé approximants exist and are uniquely determined by L, M and the first $L+M+1$ coefficients of the Taylor series of B. Padé approximants can be used to extract the values of a function B from its Taylor series (18) far beyond the radius of convergence of the series. They can be calculated by first solving a set of linear equations for the denominator coefficients b_i, and then using simple formulae to compute the numerator coefficients a_i. For convergence studies and numerical calculation of Padé approximants see [2, 3, 4, 8, 12].

In the examples of the following section the denominator coefficients have been found by Gaussian elimination with full pivoting. In all cases, in the solution of the Padé problems as well as in the recursive calculation of the Taylor coefficients $d_{k,r}$, double precision complex arithmetic was used.

3 Numerical results and comparison with experimental data

We present a number of applications, some of which have repeatedly been considered in the literature, to demonstrate the accuracy and wide applicability of our algorithms. We begin with two perfectly conducting gratings, and then we tabulate some results for a dielectric grating with real dielectric constant. Finally, comparisons with some experimental data for lossy metallic gratings and for wavelengths ranging from microwaves to ultraviolet are given.

In Tables 1a and 1b we present values for the efficiencies of a perfectly conducting sinusoidal grating

$$f(x) = \frac{h}{2}\cos(2\pi x/d) = \frac{h}{2}\cos(Kx)$$

for TE and TM polarization, respectively. The incoming wave is normally incident with wavelength-to-period ratio $\lambda/d = 0.4368$. In this configuration there are five propagating modes: $U^+ = \{0, \pm 1, \pm 2\}$. The efficiencies were computed using [32/32] Padé approximants; the computing time in a Sparc Station IPX was of about one minute for either Table 1a or 1b. The error in the energy relation (2) is denoted by

$$\epsilon = 1 - \sum_{n \in U^+} e_n.$$

Table 1a.					Table 1b.				
h/d	e_0	e_1	e_2	ϵ	h/d	e_0	e_1	e_2	ϵ
0.00	1.000	0.000	0.000	0.0E+00	0.00	1.000	0.000	0.000	0.0E+00
0.05	0.786	0.105	0.002	2.2E-16	0.05	0.743	0.125	0.004	4.4E-16
0.10	0.337	0.310	0.021	-5.6E-16	0.10	0.263	0.319	0.050	-2.2E-16
0.15	0.030	0.403	0.082	0.0E+00	0.15	0.012	0.313	0.180	-7.8E-16
0.20	0.051	0.299	0.176	-2.2E-16	0.20	0.031	0.126	0.359	-7.8E-16
0.25	0.266	0.110	0.257	2.0E-15	0.25	0.050	0.001	0.474	4.7E-15
0.30	0.423	0.012	0.277	2.3E-12	0.30	0.000	0.071	0.429	-1.0E-13
0.35	0.415	0.062	0.230	3.6E-10	0.35	0.194	0.164	0.239	-1.3E-10
0.40	0.337	0.170	0.162	1.8E-08	0.40	0.711	0.083	0.061	1.6E-09
0.45	0.317	0.211	0.131	3.5E-07	0.45	0.941	0.009	0.020	7.7E-07
0.50	0.355	0.161	0.161	2.7E-06	0.50	0.605	0.146	0.052	2.4E-05
0.55	0.355	0.101	0.222	-6.2E-06	0.55	0.199	0.344	0.057	3.0E-04
0.60	0.290	0.100	0.255	-3.6E-04	0.60	0.196	0.380	0.023	2.0E-03
0.65	0.259	0.136	0.233	-4.0E-03	0.65	0.528	0.216	0.024	6.3E-03
0.70	0.355	0.135	0.175	-2.6E-02	0.70	0.638	0.048	0.136	5.3E-03

Table 1: Efficiencies for a perfectly conducting sinusoidal grating under normal incidence with a wavelength-to-period ratio $\lambda/d = 0.4368$: [32/32] Padé approximants. Table 1a.: TE polarization; Table 1b.: TM polarization.

The case treated in Table 1 has often been used as a test for diffraction problems solvers. Our results, while more accurate, are in agreement with results presented previously. For example, Van Den Berg [26] and Pavageau and Bousquet [21] considered this problem for values of h/d ranging, from 0.3 to 0.56. They report errors of the order of 10^{-5} for a ratio of 0.3 and of order 10^{-3} for ratios of 0.4 and .56. Our own integral code, which was written following prescriptions in [15, 16], yields results of an accuracy comparable, or slightly better, to those of Van den Berg and Pavageau and Bousquet. For very deep gratings (ratios of 0.7 and beyond) our method in its present form breaks down due to numerical ill conditioning, while the integral method continues to give results with a relative error of the order of a few percent. Thus, for such gratings, the integral method is to be preferred.

Tables 2a and 2b correspond, respectively, to the TE and TM modes for the grating

$$y = \frac{h}{2} g(2\pi x/d)$$

where g is the echelette profile

$$g(x) = \begin{cases} -\frac{2x}{\pi} - 2 & \text{if } -\pi \leq x \leq -\frac{\pi}{2} \\ \frac{2x}{\pi} & \text{if } -\frac{\pi}{2} \leq x \leq \frac{\pi}{2} \\ -\frac{2x}{\pi} + 2 & \text{if } \frac{\pi}{2} \leq x \leq \pi. \end{cases} \tag{19}$$

The echelette profile (19) was approximated by its truncated Fourier series

$$\sum_{r=-F}^{F} C_{1,r} e^{iKrx}$$

with $F = 10$. The computing time, again in a Sparc Station IPX, was of about 30 seconds for Table 2a and of 60 seconds for Table 2b.

Table 2a.					Table 2b.				
h/d	e_0	e_1	e_2	ϵ	h/d	e_0	e_1	e_2	ϵ
0.00	1.000	0.000	0.000	0.0E+00	0.00	1.000	0.000	0.000	0.0E+00
0.05	0.856	0.071	0.001	-2.2E-16	0.05	0.826	0.085	0.003	-2.2E-16
0.10	0.515	0.230	0.012	-2.2E-16	0.10	0.447	0.241	0.035	-2.2E-16
0.15	0.180	0.358	0.052	-5.0E-15	0.15	0.134	0.296	0.137	-7.2E-15
0.20	0.012	0.366	0.128	-1.6E-11	0.20	0.011	0.195	0.299	3.1E-11
0.25	0.029	0.261	0.224	-5.0E-09	0.25	0.001	0.049	0.451	1.2E-08
0.30	0.136	0.125	0.307	-3.1E-07	0.30	0.001	0.002	0.497	8.6E-07
0.35	0.230	0.043	0.342	6.1E-07	0.35	0.072	0.070	0.394	2.8E-05
0.40	0.285	0.041	0.316	-1.4E-05	0.40	0.356	0.114	0.208	5.4E-04
0.45	0.348	0.080	0.246	-2.6E-04	0.45	0.721	0.059	0.084	6.0E-03
0.50	0.459	0.102	0.167	-2.4E-03	0.50	0.812	0.044	0.070	3.8E-02

Table 2: Efficiencies for a perfectly conducting symmetric echelette grating under normal incidence with a wavelength-to-period ratio $\lambda/d = 0.4368$: [12/12] Padé approximants; $F = 10$, $q_0 = 100$. Table 2a.: TE polarization; Table 2b.: TM polarization.

In Table 3 we consider a sinusoidal dielectric grating of period $1\mu m$. The grating has a refractive index $\nu_0 = 2$, and is illuminated, under normal incidence, with light of wavelength $\lambda = 0.83\mu m$. In this table, R and T represent the sums of the reflected and transmitted efficiencies, respectively. This case was treated in [10]. There, the authors used an integral equation formulation, and report the following values of R and T for $h = 0.2\mu m$:

$$R = 0.117274,$$

$$T = 0.882759$$

and

$$\epsilon = 1 - (T + R) = 3.3 \times 10^{-5};$$

compare Table 3a.

Table 3a.				Table 3b.			
h/d	R	T	ϵ	h/d	R	T	ϵ
0.00	0.111111	0.888889	-2.2E-16	0.00	0.111111	0.888889	-2.2E-16
0.10	0.114926	0.885074	0.0E+00	0.10	0.104046	0.895954	-2.2E-16
0.20	0.117282	0.882718	0.0E+00	0.20	0.086355	0.913645	0.0E+00
0.30	0.104871	0.895129	1.6E-14	0.30	0.062807	0.937193	-1.6E-12
0.40	0.080184	0.919816	9.8E-11	0.40	0.039117	0.960883	-1.1E-08
0.50	0.055902	0.944098	1.0E-07	0.50	0.025636	0.974363	-6.5E-07
0.60	0.038983	0.961015	-1.3E-06	0.60	0.023655	0.976517	1.7E-04
0.70	0.029619	0.969848	-5.3E-04	0.70	0.021333	0.982000	3.3E-03
0.80	0.024083	0.972233	-3.7E-03	0.80	0.016013	0.999951	1.6E-02

Table 3: Reflected and transmitted energies for a sinusoidal grating with index of refraction $\nu_0 = 2$, under normal incidence with a wavelength-to-period ratio $\lambda/d = 0.83$: [20/20] Padé approximants. Table 3a.: TE polarization; Table 3b.: TM polarization.

In what follows we present efficiency curves that correspond to configurations for which experimental data is available in the literature. For simplicity, we have used examples which have been reported in the review article [18].

Figure 1 corresponds to early experiments of Deleuil [9] in the microwave region. The profile is triangular, and the configuration is Littrow in order 1; the parameters are given in the caption. We have assumed, as in [18], a perfectly conducting grating, and we have approximated the grating profile by its Fourier series with fifteen modes. Higher order Fourier approximations lead to identical graphs. [12/12] Padé approximants were used. We observe somewhat better agreement with the experimental data than that reported in [18, p. 161]. Figure 2 corresponds again to a triangular profile in Littrow mount. In this case, infrared radiation is used. The parameters used in our numerics are identical with those in Figure 1. The Wood anomalies at $\lambda/d = .64$ and $\lambda/d = .68$ are very well resolved (compare [18, p. 164]).

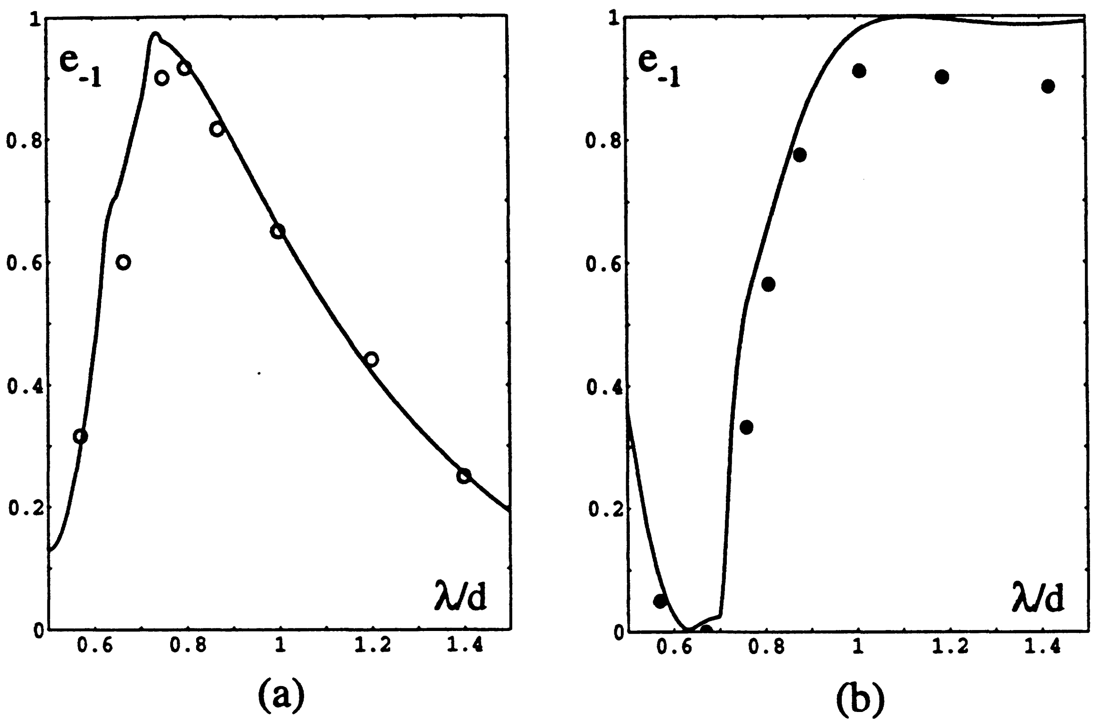

Figure 1: Efficiency curves for a perfectly conducting ruled grating (blaze angle= 37°, included angle= 94°, deviation angle= 8.9°) in the microwave region: (a) TE polarization; (b) TM polarization.

Figure 3 corresponds to an 830 groove/mm sinusoidal holographic silver grating in the visible range as a function of the incidence. Close agreement with the experimental curves of [13] is observed; see also [18, p. 166], were similar agreement was found. Finally, in Figure 4 we show experimental values and theoretical curves for a 158 groove/mm aluminum ruled (triangular) grating in near UV. Values of the refractive indices of aluminum were taken from [1]. The bottom, intermediate and top curves in Figure 4 correspond to Fourier representation of the profile by using 15, 21 and 25 Fourier modes respectively. We note that the representation with 15 modes yields values that match the experimental results best. Quite possibly, the actual grating profile contains rounded rather than sharp vertices, thus explaining the better match with results obtained by assuming a lower order Fourier series. A theoretical curve in the region $0.2 \leq \lambda \leq 0.6$ is given in [18, p. 170], showing qualitative agreement with these experimental results.

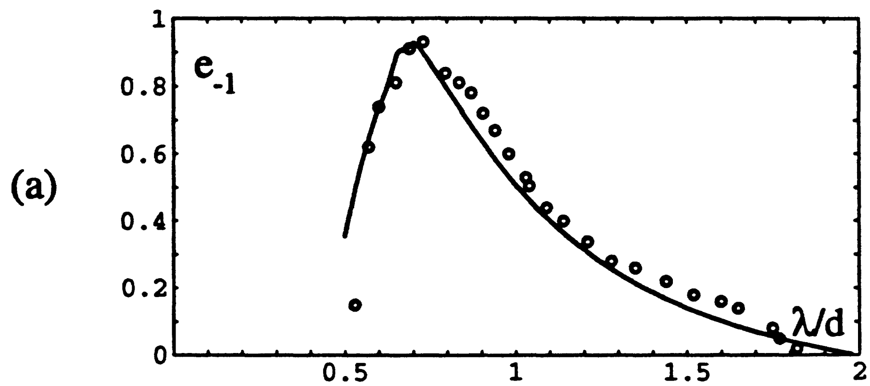

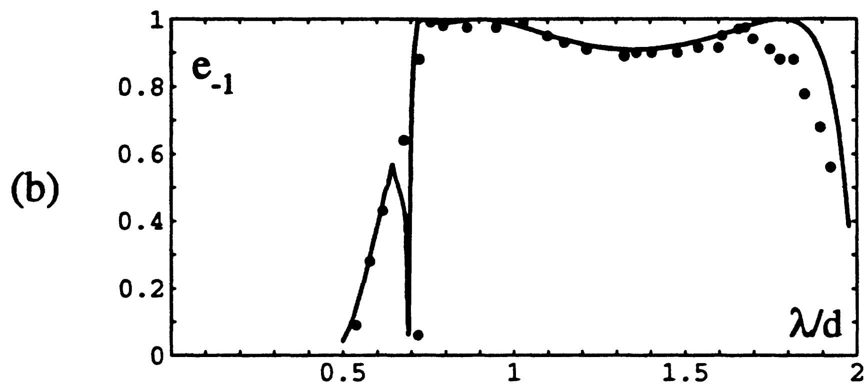

Figure 2: Efficiency curves of a 26.75° blaze angle perfectly conducting echelette grating in the infrared (angular deviation = 3.5° between incident and −1 order diffracted waves): (a) TE polarization; (b) TM polarization.

4 Singularities, enhanced convergence and Padé approximants

It is well known that, rather generally, the singularities of the Padé approximants approach the singularities of the function they approximate [2]. In Figure 5 we show the location of the zeroes of the numerators and denominators of the [28/28] and [48/48] Padé approximants to the Rayleigh coefficient $B_1(\delta)$ for the perfectly conducting grating

$$f_\delta(x) = \delta(e^{i2\pi x} + e^{-i2\pi x}) = 2\delta\cos(2\pi x)$$

under normal incidence with wavelength $\lambda = .4368$. This example was considered in Table 1; note the correspondence

$$h/d = 4\delta. \tag{20}$$

In this figure, a circle ('o') represents a zero of the denominator, which is a singularity of the approximant provided it is not crossed out by a corresponding zero ('x') in the numerator. We see that no singularities occur on the real axis, as expected from our theoretical discussion. Indeed,

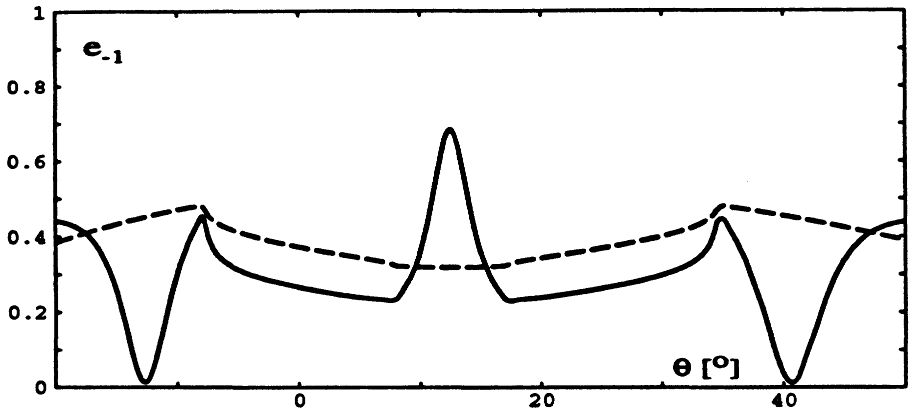

Figure 3: Efficiency of an 830 groove/mm sinusoidal holographic silver grating in the visible ($\lambda = 0.521\mu m$), as a function of the incidence. Dashed: TE polarization; Solid: TM polarization.

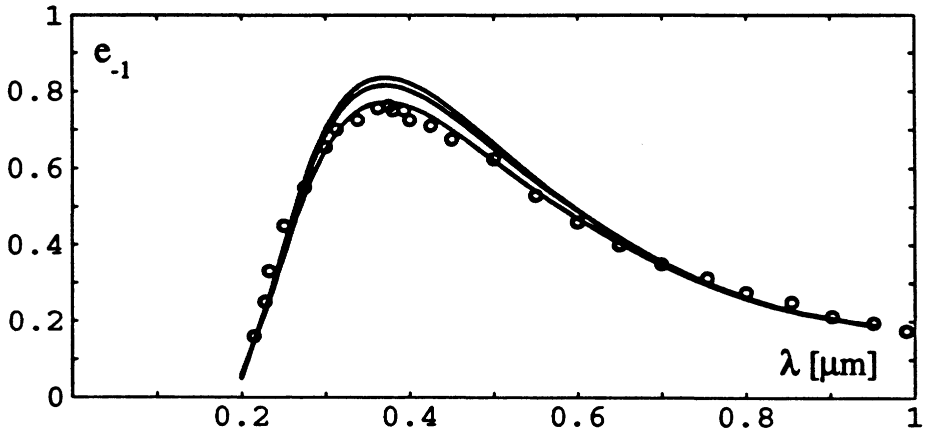

Figure 4: TE efficiency curve for a 158 l/mm aluminum ruled grating (blaze angle= 1.66°, included angle= 90°, deviation angle= 3.5°) in near UV.

Padé approximants provide us with an approximation to the domain of analyticity of the diffracted fields. (Figure 5 corresponds to the Rayleigh coefficients $B_1 = B_1(\delta)$. Very similar pictures are obtained for the amplitudes B_2 and B_3 and for approximants of other orders).

A domain of analyticity C which resembles the one suggested by Figure 5 was proposed in [6] (see region C in Figure 6 below). Figure 6 lead us to devise a summation mechanism, enhanced convergence, which is based on conformal transformations. As we have said, the method of enhanced convergence permitted us to apply our analytic approach to many practical situations. It is apparent now, however, that better results are to be obtained by means of Padé approximation (compare Tables 1a,b of this paper and Tables 2a,b in [6]). As it will be argued below, a combination of both summation methods could further improve the quality of our algorithms. Towards this end we discuss, in what follows, some connections that exist among singularity distributions, such as those

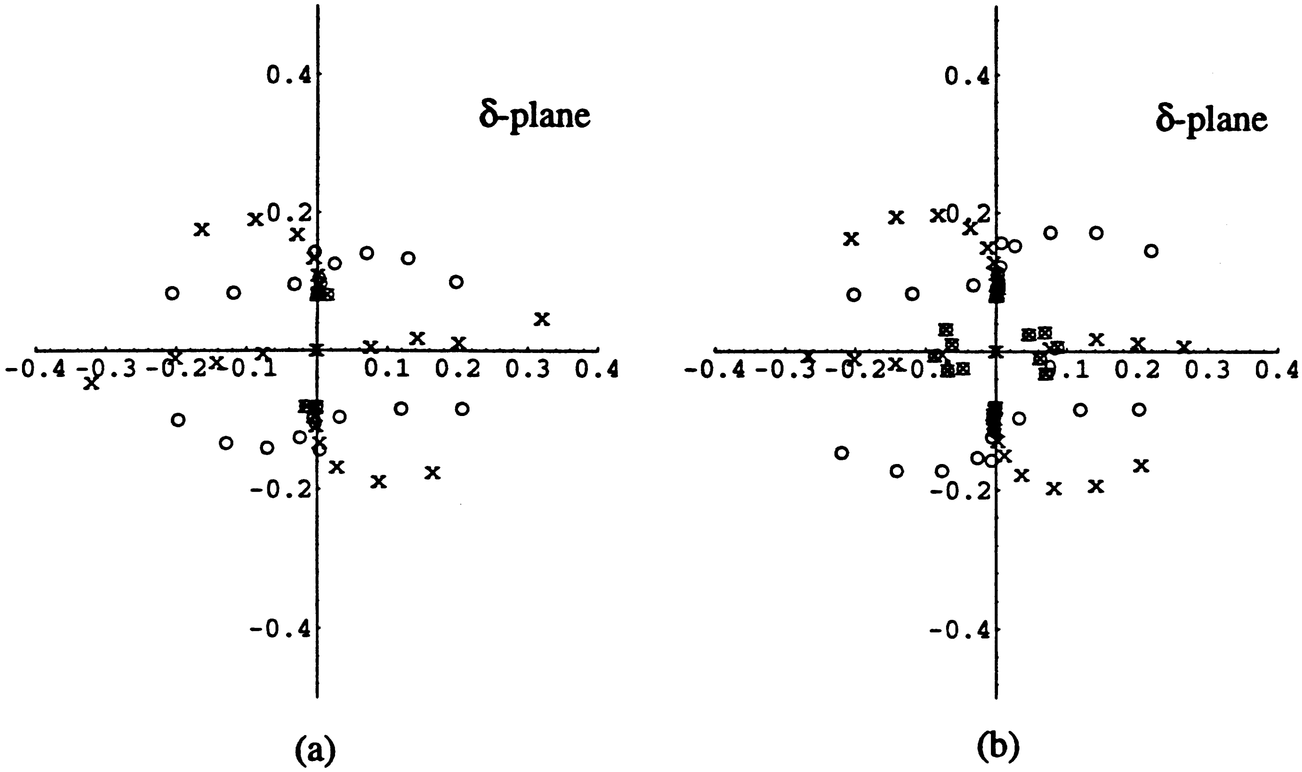

Figure 5: Poles (o) and zeros (x) of the Padé approximants of $B_1(\delta)$: (a) [28/28]-approximant and (b) [48/48]-approximant.

in Figure 5, and the efficiency of the methods of enhanced convergence and Padé approximation.

Given a function $B(\delta)$ and a complex number δ_0, the method of enhanced convergence uses conformal transformations to produce an arrangement of the singularities of B and the point δ_0, so that a truncated Taylor series can be used to calculate $B(\delta_0)$. For example, we know from the theory in §2.1 (see also Figure 5) that the electromagnetic field, and therefore, the Rayleigh coefficients $B_r^{\pm}(\delta)$, are analytic functions of δ in a neighborhood of the real axis in the complex δ-plane. The width of this neighborhood is not necessarily uniform along the real axis, as suggested by our representation C in Figure 6 of the region of analyticity of $B_r^{\pm}(\delta)$. Suppose one wishes to compute the function $B(\delta)$ at a point δ_0 which lies outside the circle of convergence D of the Taylor series of B around $\delta = 0$ (see Figure 6). The series is divergent at δ_0. If we consider, however, the composition of B with a conformal transformation,

$$\xi = g(\delta),$$

the singularities and the point $\xi_0 = g(\delta_0)$ at which the function is sought will show a different arrangement *in the ξ-plane* and, possibly, ξ_0 will lie inside the circle of convergence of the composite function $B(g^{-1}(\xi))$. If so, a truncated Taylor series of the composite function can be summed to yield the value $B(\delta_0)$. Even if δ_0 lies inside the circle of convergence D, this procedure may result

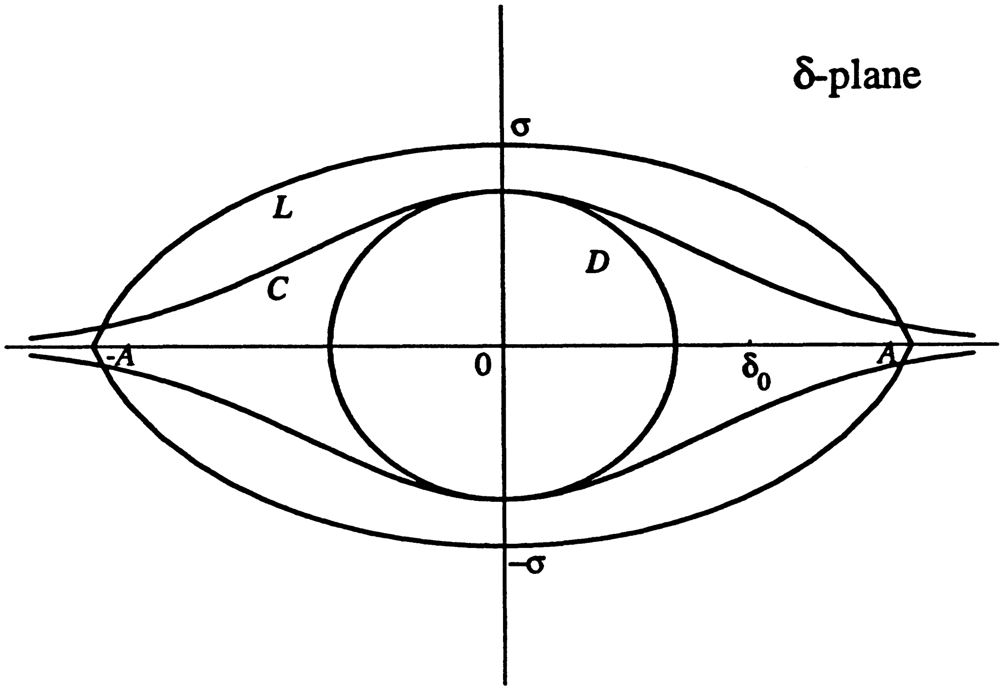

Figure 6: The region C of analyticity of the Rayleigh coefficients $B_r^{\pm}(\delta)$ and the lens-shaped region L that is conformally transformed onto the right-half plane via $g(\delta) = (\frac{A-\delta}{A+\delta})^{\alpha}$.

in improved convergence rates [6, 7].

In [6] we used the transformation

$$\xi = g(\delta) = (\frac{A-\delta}{A+\delta})^{\alpha}$$

to map the elongated region L in Figure 6, which consists of the intersection of two discs, onto the right-half ξ-plane. The parameters σ and A in Figure 6 control the distribution of singularities of the composite functions

$$B_r(g^{-1}(\xi)). \tag{21}$$

These parameters can be chosen in such a way that the composite series about $\xi = 1$ converges at the value of ξ that corresponds to any given real value of δ. Indeed, given any $\delta \in \mathbf{R}$, taking A large enough we will have $\delta \in L$. Then, taking σ small enough we will have $L \subseteq C$, and, therefore, the composite maps (21) will be analytic in a circle about $\xi = 1$ that contains $g(\delta)$. The optimal value of the parameters, however, should be chosen so as to obtain the fastest convergence for the series of (21). If the complex numbers δ_j denote singularities of the functions $B_r(\delta)$, then A and σ should minimize, for any given δ, the expression

$$\max_j \left(\frac{|g(\delta) - 1|}{|g(\delta_j) - 1|} \right), \tag{22}$$

see [7].

A pair of optimal parameters A and σ can be obtained, without any knowledge of the set of singularities of B_r, simply by seeking parameters that yield the fastest numerical convergence. In [6] we observed that the convergence rates are rather insensitive to changes in the parameter A, provided A is large enough, say $A = 9$. In contrast, the convergence rates were observed to be very sensitive even to small changes in the parameter σ. In [6] we chose $\sigma = .13$, as we observed that best convergence rates were obtained for $\sigma = .13 \pm .01$.

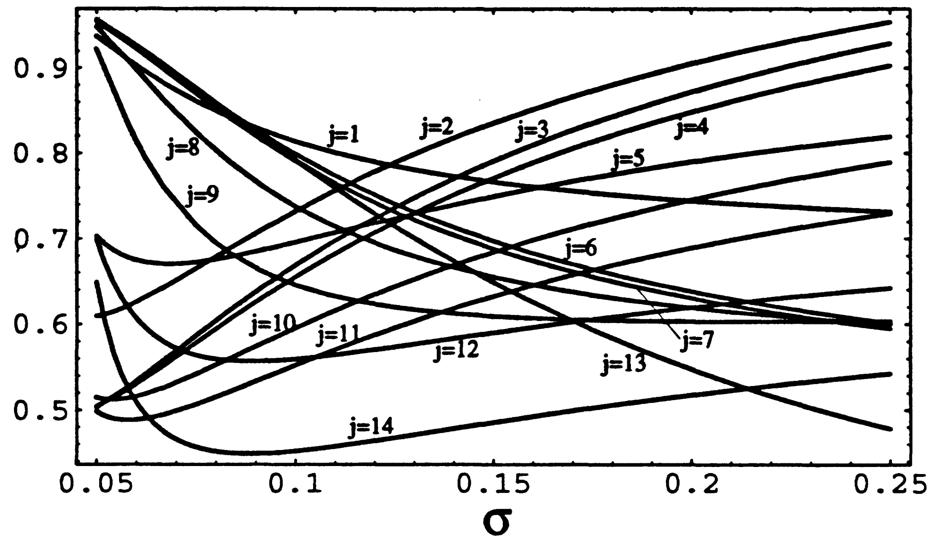

Figure 7: Plot of $\frac{|g(\delta=0.1)-1|}{|g(\delta_j)-1|}$ as functions of σ.

On the other hand, we can calculate the optimal value of σ simply by minimizing the expression (22), where δ_j are the poles shown in Figure 5. It is not hard to see that only the 14 poles which appear on the right hand plane need to be considered. In Figure 7 we show plots of $\frac{|g(\delta)-1|}{|g(\delta_j)-1|}$ for $j = 1, \ldots, 14$ as functions of σ for $\delta = 0.1$ (which corresponds to a height to period ratio of $h/d = 0.4$, see (20)). We see that expression (22) is minimized at about $\sigma = .123$, in agreement with our previous estimates. This agreement constitutes an important consistency check in our theory.

As we have said above, enhanced convergence can be used in combination with Padé approximants. Indeed, we have shown [7] that the relative arrangement of the singularities of an analytic function is closely related to the numerical conditioning of the corresponding Padé approximation. A conformal change of variables on a function $B(\delta)$ can lead to a dramatic improvement in the conditioning of the corresponding Padé problem. And, interestingly, conformal maps which are optimal in the context of enhanced convergence, also lead to optimal conditioning in Padé approximation. Since the main numerical weakness of Padé approximation is its ill conditioning, it is reasonable to expect that its use in conjunction with enhanced convergence would lead to improvement in the calculation of the diffraction efficiencies. A great deal of improvement has been obtained, as a matter of fact, by using this idea in some simple approximation problems [7]. However, there is a requisite that needs to be met: one needs to use accurate values of the series of the composite functions.

Composition of the corresponding series will not do, as such operation results in a loss of significant digits which degrades the numerics and yields no substantial improvement in the calculated values. Thus, important progress would be made if an appropriate conformal mapping g, together with an adequate method for the calculation of the derivatives of the composite functions (21) were found.

Acknowledgments. OB gratefully acknowledges support from NSF through grant No. DMS-9200002. This work was partially supported by the Army Research Office and the National Science Foundation through the Center for Nonlinear Analysis.

References

[1] *American Institute of Physics Handbook*, 3rd. Edition, ed. D. E. Gray, McGraw-Hill, New York (1981).

[2] Baker, G. A. and Graves–Morris, P., *Padé Approximants. Part I: Basic Theory,* Addison–Wesley, Massachusetts (1981).

[3] Baker, G. A. and Graves–Morris, P., *Padé Approximants. Part II: Extensions and Applications,* Addison–Wesley, Massachusetts (1981).

[4] Brezinski, C., *Procedures for estimating the error in Padé approximation,* Mathematics of Computation **53**, 639–648 (1965).

[5] Bruno, O. P. and Reitich, F., *Solution of a boundary value problem for Helmholtz equation via variation of the boundary into the complex domain,* to appear in Proc. Roy. Soc. Edinburgh.

[6] Bruno, O. P. and Reitich, F., *Numerical solution of diffraction problems: a method of variation of boundaries,* to appear in J. Opt. Soc. Amer. A.

[7] O. Bruno and F. Reitich, *Approximation of analytic functions: a method of enhanced convergence,* Preprint (1992).

[8] Cabay, S. and Choi, D., *Algebraic computations of scaled Padé fractions,* SIAM J. Comput. **15**, 243–270 (1986).

[9] Deleuil, R., *Réalisation et utilisation d'un appareillage destiné à l'étude des dioptres irreéguliers et des réseaux en ondes millimétriques,* Optica Acta **16**, 23–35 (1969).

[10] D. C. Dobson, and J. A. Cox, *An integral equation method for biperiodic diffraction structures,* SPIE, **1545**, 106–113 (1991).

[11] Glytsis, E. N. and Gaylord, T. K., *Three-dimensional (vector) rigorous coupled-wave analysis of anisotropic grating diffraction,* J. Opt. Soc. Amer. A **7**, 1399–1420 (1990).

[12] Graves–Morris, P., *The numerical calculation of Padé approximants,* Lecture Notes in Mathematics **765**, ed. L. Wuytack, 231–245 (1979).

[13] Hutley, M. C. and Bird, V. M., *A detailed experimental study of the anomalies of a sinusoidal diffraction grating,* Optica Acta **20**, 771–782 (1973).

[14] Ikuno, H. and Yasuura, K. *Improved point-matching method with applications to scattering from a periodic surface,* IEEE Trans. Antennas Propag. **AP-21**, 657–662 (1973).

[15] Maystre, D., *Integral Methods,* in Electromagnetic Theory of Gratings, ed. R. Petit, Springer, Berlin (1980).

[16] Maystre, D., *Rigorous vector theories of diffraction gratings,* in Progress in Optics, ed. E. Wolf, North Holland, Amsterdam (1984).

[17] Maystre, D. and Nevière, M., *Electromagnetic theory of crossed gratings,* J. Optics **9**, 301–306 (1978)

[18] Maystre, D., Nevière, M., and Petit, R. *Experimental verifications and applications of the theory,* in Electromagnetic Theory of Gratings, ed. R. Petit, Springer, Berlin (1980).

[19] Meecham, W. C., *On the use of the Kirchoff approximation for the solution of reflection problems,* J. Rat. Mech. Anal. **5**, 323–334 (1956).

[20] Millar, R. F., *On the Rayleigh assumption in scattering by a periodic surface II,* Proc. Camb. Phil. Soc. **69**, 217–225 (1971).

[21] Pavageau, J., Bousquet, J.,*Diffraction par un réseau conducteur nouvelle méthode de résolution,* Optica Acta **17**, 469–478 (1970).

[22] Petit, R., ed., *Electromagnetic Theory of Gratings,* Springer, Berlin (1980).

[23] Lord Rayleigh, *The theory of sound, vol.2,* Dover, New York (1945).

[24] Talbot, D., Titchener, J. B. and Willis, J. R., *The reflection of electromagnetic waves from very rough interfaces,* Wave Motion **12**, 245–260 (1990).

[25] Uretsky, J. L., *The scattering of plane waves from periodic surfaces,* Ann. Phys. **33**, 400–427 (1965).

[26] Van den Berg, P. M., *Diffraction theory of a reflection grating,* Appl. Sci. Res. **24**, 261–293 (1971).

[27] Wait, J. R., *Perturbation analysis for reflection from two-dimensional periodic sea waves,* Radio Science **6**, 387–391 (1971).

Center for Nonlinear Analysis
Report Series • Complete List

Nonlinear Analysis Series

No.

91-NA-001 [ ] Lions, P.L., **Jacobians and Hardy spaces**, June 1991

91-NA-002 [ ] Giga, Y. and Soto, M.-H., **Generalized interface evolution with the Neumann boundary condition**, July 1991

91-NA-003 [ ] Soner, H.M. and Souganidis, P.E., **Uniqueness and singularities of cylindrically symmetric surfaces moving by mean curvature**, July 1991

91-NA-004 [ ] Coleman, B.D., Marcus, M. and Mizel, V.J., **On the Thermodynamics of periodic phases**, August 1991

91-NA-005 [ ] Gurtin, M.E. and Podio-Guidugli, P., **On the formulation of mechanical balance laws for structured continua**, August 1991

91-NA-006 [ ] Gurtin, M.E. and Voorhees, P., **Two-phase continuum mechanics with mass transport and stress**, August 1991

91-NA-007 [ ] Fried, E., **Non-monotonic transformation kinetics and the morphological stability of phase boundaries in thermoelastic materials**, September 1991

91-NA-008 [ ] Gurtin, M.E., **Evolving phase boundaries in deformable continua**, September 1991

91-NA-009 [ ] Di Carlo, A., Gurtin, M.E., and Podio-Guidugli, P., **A regularized equation for anisotropic motion-by-curvature**, September 1991

91-NA-010 [ ] Kinderlehrer, D. and Ou, B., **Second variation of liquid crystal energy at $x/|x|$**, August 1991

91-NA-011 [ ] Baughman, L.A. and Walkington, N., **Co-volume methods for degenerate parabolic problems**, August 1991

91-NA-012 [ ] James, R.D. and Kinderlehrer, D., **Frustration and microstructure: An example in magnetostriction**, November 1991

91-NA-013 [ ] Angenent, S.B. and Gurtin, M.E., **Anisotropic motion of a phase interface**, November 1991

92-NA-001 [ ] Nicolaides, R.A. and Walkington, N.J., **Computation of microstructure utilizing Young measure representations,** January 1992

92-NA-002 [ ] Tartar, L., **On mathematical tools for studying partial differential equations of continuum physics: H-measures and Young measures,** January 1992

92-NA-003 [ ] Bronsard, L. and Hilhorst, D., **On the slow dynamics for the Cahn-Hilliard equation in one space dimension,** February 1992

92-NA-004 [ ] Gurtin, M.E., **Thermodynamics and the supercritical Stefan equations with nucleations,** March 1992

92-NA-005 [ ] Antonic, N., **Memory effects in homogenisation linear second order equation,** February 1992

92-NA-006 [ ] Gurtin, M.E. and Voorhees, P.W., **The continuum mechanics of coherent two-phase elastic solids with mass transport,** March 1992

92-NA-007 [ ] Kinderlehrer, D. and Pedregal, P., **Remarks about gradient Young measures generated by sequences in Sobolev spaces,** March 1992

92-NA-008 [ ] **Workshop on Shear Bands,** March 23-25, 1992 (Abstracts), March 1992

92-NA-009 [ ] Armstrong, R. W., **Microstructural/Dislocation Mechanics Aspects of Shear Banding in Polycrystals,** March 1992

92-NA-010 [ ] Soner, H. M. and Souganidis, P. E., **Singularities and Uniqueness of Cylindrically Symmetric Surfaces Moving by Mean Curvature,** April 1992

92-NA-011 [ ] Owen, David R., Schaeffer, Jack, andWang, Keming, **A Gronwall Inequality for Weakly Lipschitzian Mappings,** April 1992

92-NA-012 [ ] Alama, Stanley and Li, **Yan Yan, On "Multibump" Bound States for Certain Semilinear Elliptic Equations,** April 1992

92-NA-013 [ ] Olmstead, W. E., Nemat-Nasser, S., and Li, L., **Shear Bands as Discontinuities,** April 1992

92-NA-014 [ ] Antonic, N., **H-Measures Applied to Symmetric Systems,** April 1992

92-NA-015 [ ] Barroso, Ana Cristina and Fonseca, Irene, **Anisotropic Singular Perturbations - The Vectorial Case,** April 1992

92-NA-016 [ ] Pedregal, Pablo, **Jensen's Inequality in the Calculus of Variations,** May 1992

92-NA-017 [ ] Fonseca, Irene and Muller, Stefan, **Relaxation of Quasiconvex Functionals in $BV(\Omega,\Re P)$ for Integrands $f(x,u,\nabla u)$,** May 1992

92-NA-018	[ ]	Alama, Stanley and Tarantello, Gabriella, **On Semilinear Elliptic Equations with Indefinite Nonlinearities**, May 1992
92-NA-019	[ ]	Owen, David R., **Deformations and Stresses With and Without Microslip**, June 1992
92-NA-020	[ ]	Barles, G., Soner, H. M., Souganidis, P. E., **Front Propagation and Phase Field Theory**, June 1992
92-NA-021	[ ]	Bruno, Oscar P. and Reitich, Fernando, **Approximation of Analytic Functions: A Method of Enhanced Convergence**, July 1992
92-NA-022	[ ]	Bronsard, Lia and Reitich, Fernando, **On Three-Phase Boundary Motion and the Singular Limit of a Vector-Valued Ginzburg-Landau Equation**, July 1992
92-NA-023	[ ]	Cannarsa, Piermarco, Gozzi, Fausto and Soner, H.M., **A Dynamic Programming Approach to Nonlinear Boundary Control Problems of Parabolic Type**, July 1992
92-NA-024	[ ]	Fried, Eliot and Gurtin, Morton, **Continuum Phase Transitions With An Order Parameter; Accretion and Heat Conduction**, August 1992
92-NA-025	[ ]	Swart, Pieter J. and Homes, Philip J., **Energy Minimization and the Formation of Microstructure in Dynamic Anti-Plane Shear**, August 1992
92-NA-026	[ ]	Ambrosio, I., Cannarsa, P. and Soner, H.M., **On the Propagation of Singularities of Semi-Convex Functions**, August 1992
92-NA-027	[ ]	Nicolaides, R.A. and Walkington, Noel J., **Strong Convergence of Numerical Solutions to Degenerate Varational Problems**, August 1992
92-NA-028	[ ]	Tarantello, Gabriella, **Multiplicity Results for an Inhomogenous Neumann Problem with Critical Exponent**, August 1992
92-NA-029	[ ]	Noll, Walter, **The Geometry of Contact, Separation, and Reformation of Continous Bodies**, August 1992
92-NA-030	[ ]	Brandon, Deborah and Rogers, Robert C., **Nonlocal Superconductivity**, July 1992
92-NA-031	[ ]	Yang, Yisong, **An Equivalence Theorem for String Solutions of the Einstein-Matter-Gauge Equations**, September 1992
92-NA-032	[ ]	Spruck, Joel and Yang,Yisong, **Cosmic String Solutions of the Einstein-Matter-Gauge Equations**, September 1992
92-NA-033	[ ]	**Workshop on Computational Methods in Materials Science (Abstracts)**, September 16-18, 1992.

92-NA-034 [ ] Leo, Perry H. and Herng-Jeng Jou, **Shape evolution of an initially circular precipitate growing by diffusion in an applied stress field**, October 1992

92-NA-035 [ ] Gangbo, Wilfrid, **On the weak lower semicontinuity of energies with polyconvex integrands**, October 1992

92-NA-036 [ ] Katsoulakis, Markos, Kossioris, Georgios T. and Retich, Fernando, **Generalized motion by mean curvature with Neumann conditions and the Allen-Cahn model for phase transitions**, October 1992

92-NA-037 [ ] Kinderlehrer, David, **Some methods of analysis in the study of microstructure**, October 1992

92-NA-038 [ ] Yang, Yisong, **Self duality of the Gauge Field equations and the Cosmological Constant**, November 1992

92-NA-039 [ ] Brandon, Deborah and Rogers, Robert, **Constitutive Laws for Pseudo-Elastic Materials**, November 1992

92-NA-040 [ ] Leo, P. H., Shield, T. W., and Bruno, O. P., **Transient Heat Transfer Effects on the Pseudoelastic Behavior of Shape-Memory Wires**, November 1992

92-NA-041 [ ] Gurtin, Morton E., **The Dynamics of Solid-Solid Phase Transitions 1. Coherent Interfaces**, November 1992

92-NA-042 [ ] Gurtin, Morton E., Soner, H. M., and Souganidis, P. E., **Anisotropic Motion of an Interface Relaxed by the Formation of Infinitesimal Wrinkles**, December 1992

92-NA-043 [ ] Bruno, Oscar P., and Fernando Reitich, **Numerical Solution of Diffraction Problems: A Method of Variation of Boundaries II. Dielectric gratings, Padé Approximants and Singularities**, December 1992

93-NA-001 [ ] Mizel, Victor J., **On Distribution Functions of the Derivatives of Weakly Differentiable Mappings**, January 1993

93-NA-002 [ ] Kinderlehrer, David, Ou, Biao and Walkington, Noel, **The Elementary Defects of the Oseen-Frank Energy for a Liquid Crystal**, January 1993

93-NA-003 [ ] Bruno, Oscar P., Reitich, Fernando, **Numerical Solutions of Diffraction Problems: A Method of Variation of Boundaries III. Doubly Periodic Gratings**, January 1993

93-NA-004 [ ] James, Richard and Kinderlehrer, David, **Theory of Magnetostriction with Applications to $Tb_xDy_{1-x}Fe_2$**, February 1993

93-NA-005 [ ] Del Piero, Gianpietro and Owen, David R., **Structured Deformations of Continua**, February 1993

93-NA-006 [ ] Cheng, Chih-Wen and Mizel, Victor J., **On the Lavrentiev Phenomenon for Autonomous Second Order Integrands**, February 1993

93-NA-007 [ ] Ma, Ling, **Computation of Magnetostrictive Materials**, February 1993

93-NA-008 [ ] James, Richard and Kinderlehrer, David, **Mathematical Approaches to the Study of Smart Materials**, February 1993

Stochastic Analysis Series

91-SA-001 [ ] Soner, H.M., **Singular perturbations in manufacturing**, November 1991

91-SA-002 [ ] Bridge, D.S. and Shreve, S.E., **Multi-dimensional finite-fuel singular stochastic control**, November 1991

92-SA-001 [ ] Shreve, S. E. and Soner, H. M., **Optimal Investment and Consumption with Transaction Costs**, September 1992